

RESEARCH ARTICLE

Use of ESI-FTICR-MS to Characterize Dissolved Organic Matter in Headwater Streams Draining Forest-Dominated and Pasture-Dominated Watersheds

Yuehan Lu^{1*}, Xiaping Li¹, Rajaa Mesfioui², James E. Bauer³, R. M. Chambers⁴, Elizabeth A. Canuel⁵, Patrick G. Hatcher²

1 Department of Geological Sciences, University of Alabama, Tuscaloosa, Alabama, United States of America, **2** Department of Chemistry and Biochemistry, Old Dominion University, Norfolk, Virginia, United States of America, **3** Aquatic Biogeochemistry Laboratory, Department of Evolution, Ecology and Organismal Biology, Ohio State University, Columbus, Ohio, United States of America, **4** Department of Biology, College of William and Mary, Williamsburg, Virginia, United States of America, **5** Department of Physical Sciences, Virginia Institute of Marine Sciences, Gloucester Point, Virginia, United States of America

* yuehan.lu@ua.edu



OPEN ACCESS

Citation: Lu Y, Li X, Mesfioui R, Bauer JE, Chambers RM, Canuel EA, et al. (2015) Use of ESI-FTICR-MS to Characterize Dissolved Organic Matter in Headwater Streams Draining Forest-Dominated and Pasture-Dominated Watersheds. PLoS ONE 10(12): e0145639. doi:10.1371/journal.pone.0145639

Editor: Jon M. Jacobs, Pacific Northwest National Laboratory, UNITED STATES

Received: June 10, 2015

Accepted: December 7, 2015

Published: December 29, 2015

Copyright: © 2015 Lu et al. This is an open access article distributed under the terms of the [Creative Commons Attribution License](https://creativecommons.org/licenses/by/4.0/), which permits unrestricted use, distribution, and reproduction in any medium, provided the original author and source are credited.

Data Availability Statement: All relevant data are within the paper and the files of Supporting Information.

Funding: This work was supported by a start-up analytical fund to YL from the Department of Geological Science at the University of Alabama and a Mellon Foundation Postdoctoral Fellow Grant from the College of William and Mary. The authors also acknowledge the HOOK's research fund and the Johnson travel fund from the Department of Geological Sciences, the University of Alabama, for providing student research and travel funds.

Abstract

Electrospray ionization Fourier transform ion cyclotron resonance mass spectrometry (ESI-FTICR-MS) has proven to be a powerful technique revealing complexity and diversity of natural DOM molecules, but its application to DOM analysis in grazing-impacted agricultural systems remains scarce. In the present study, we presented a case study of using ESI-FTICR-MS in analyzing DOM from four headwater streams draining forest- or pasture-dominated watersheds in Virginia, USA. In all samples, most formulas were CHO compounds (71.8–87.9%), with other molecular series (CHOS, CHON, CHONS, and CHOP (N, S)) accounting for only minor fractions. All samples were dominated by molecules falling in the lignin-like region ($H/C = 0.7–1.5$, $O/C = 0.1–0.67$), suggesting the predominance of allochthonous, terrestrial plant-derived DOM. Relative to the two pasture streams, DOM formulas in the two forest streams were more similar, based on Jaccard similarity coefficients and nonmetric multidimensional scaling calculated from Bray-Curtis distance. Formulas from the pasture streams were characterized by lower proportions of aromatic formulas and lower unsaturation, suggesting that the allochthonous versus autochthonous contributions of organic matter to streams were modified by pasture land use. The number of condensed aromatic structures (CAS) was higher for the forest streams, which is possibly due to the controlled burning in the forest-dominated watersheds and suggests that black carbon was mobilized from soils to streams. During 15-day biodegradation experiments, DOM from the two pasture streams was altered to a greater extent than DOM from the forest streams, with formulas with H/C and O/C ranges similar to protein ($H/C = 1.5–2.2$, $O/C = 0.3–0.67$), lipid ($H/C = 1.5–2.0$, $O/C = 0–0.3$), and unsaturated hydrocarbon ($H/C = 0.7–1.5$, $O/C = 0–0.1$) being the most bioreactive groups. Aromatic compound formulas including CAS were preferentially removed during combined light+bacterial incubations, supporting the contention

Competing Interests: The authors have declared that no competing interests exist.

that black carbon is labile to light alterations. Collectively, our data demonstrate that headwater DOM composition contains integrative information on watershed sources and processes, and the application of ESI-FTICR-MS technique offers additional insights into compound composition and reactivity unrevealed by fluorescence and stable carbon isotopic measurements.

Introduction

Dissolved organic matter (DOM) in streams and rivers is derived from both watershed and aquatic contributions, containing information integrating various biological sources and ecological processes. As a complex mixture containing a multitude of components with varied composition and reactivity, DOM plays a pivotal role in a variety of biogeochemical processes within aquatic environments, including altering light regime, providing energy and substrate to heterotrophic food webs, and influencing the forms of metal pollutants. Historically, the chemical characteristics of natural DOM have been analyzed mostly through bulk methods, including element compositions (particularly DOC:DON molecular ratios), stable carbon isotopes of DOC ($\delta^{13}\text{C}$ -DOC), and optical properties which can generate a series of source and reactivity indices based on fluorescence and absorption [1–4]. These techniques capture DOM as a whole but can be biased from averaging DOM constituents of various characteristics. Using such methods, molecular-level understanding of DOM remains limited because low-resolution instrumental approaches cannot separate and identify complex molecules in natural DOM.

Fourier transform ion cyclotron resonance mass spectrometry (FTICR-MS) analysis is increasingly recognized over the past decade as a powerful instrumental approach for characterizing DOM at the molecular level [5]. FTICR-MS provides unparalleled resolution for identification of ionized organic compounds, and it can be coupled with atmospheric pressure electrospray ionization (ESI) technique to ionize water-soluble, hydrophilic molecules with no or negligible fragmentation [6–8]. Unsurprisingly, ESI-FTICR-MS has been more frequently used to obtain more detailed and accurate compositional information on natural DOM. For example, Sleighter and Hatcher [9], using ESI-FTICR-MS, successfully resolved thousands of DOM components along a river-estuary-coastal ocean transect in lower Chesapeake Bay. Through comparing FTICR-MS molecular families to fluorescence components derived from excitation emission matrix-parallel factor analysis (EEM-PARAFAC) in 22 freshwater samples, Stubbins and colleagues [8] show that fluorescence components represented less than half of the total number of formulas identified using FTICR-MS, furthering demonstrating the need to apply this technique to various systems for acquiring more robust information about the diversity of natural DOM compounds.

A few recent studies have applied FTICR-MS to characterizing DOM in soils and natural waters across a range of ecosystems [10–11]. To date, few FTICR-MS studies have been focused on human-impacted watersheds, especially considering high spatiotemporal variability observed across geographic regions and ecosystem types. In particular, detailed, molecular-level chemical characterizations of DOM exported from grazing-impacted systems remain scarce, although grazed lands account for around 45% of non-Federal rural lands in US. In the present case study, we employed ESI-FTICR-MS to compare the composition of DOM from temperate headwater streams draining watersheds dominated by forest and pasture land use. Additionally, we conducted laboratory microbial and photochemical incubations to assess how DOM composition influences the biodegradability and photodegradability. The study sites

included four temperate streams of similar lithological and meteorological variables, and samples were collected at base flow. This sampling strategy minimizes DOM variations related to geological, climatic, and hydrological differences but highlights those more due to watershed land use differences.

Materials and Methods

Sample collection, filtration and incubation

Our study site included four headwater streams located 1–6 km apart, within the watershed of Mattaponi River, a tributary of the York River discharging to the Chesapeake Bay, Virginia, USA (Fig 1). Two of the streams (F1, F2) were situated within watersheds dominated by oak-pine forest (hereafter referred to as “forest streams”); the other two streams, P1 and P2, drained pasture-dominated watersheds (hereafter referred to as “pasture streams”), where pastures were rotated annually between warm-season grasses (May–October) and cool-season grasses (November–April) under the management of a local cattle farm. The study was carried out on private land, and the owners gave permission to conduct this study on the sites.

All streams were sampled during base flow conditions in November, 2009. During the sampling, a suite of *in situ* parameters was measured (Table 1). Stream water samples were collected in 20 l acid-cleaned polycarbonate carboys (soaked in 10% acid for > 24 h and rinsed extensively with Nanopure water) using a Masterflex® E/S™ portable sampler (Cole-Parmer) equipped with acid-cleaned silicone tubing. After collection, samples were stored on ice in the dark for up to 6 hours until being filtered in the lab. Living and non-living particulate materials were removed by filtering water through GF/F glass fiber filters (nominal pore size 0.7 μm, pre-combusted at 500°C for 5 h) [3]. Laboratory incubations were started immediately after the filtration process. All incubations lasted 15 days at 22±2°C, including two treatment types: 1) bacteria-only treatment (i.e., 0.7 μm filtrate under dark conditions) for all the samples, and 2) combined light+bacteria treatment (i.e., 0.7 μm filtrate under light conditions) only for samples from the pasture streams. Combined light+bacteria incubations were performed in 500 ml quartz flasks on a rotating light table, with the spectra of the light source having similar characteristics to that of natural sunlight for UV wavelengths between 295 and 365 nm. The irradiance was approximately one third of seasonally averaged daily solar irradiance in shallow water at 40°N [12], and thus the amount of UV exposure during the 15 days of 24 h light incubations was similar to 10 days of 12 h daylight at the sampling sites. Dark incubations were conducted in one-liter amber borosilicate glass bottles, which were covered by dark bags to further prevent light penetration. Throughout the incubations, subsamples were collected at the beginning and end of the incubations (T₀ and T₁₅, respectively) as well as four to six intermediate time points for the evaluation of DOC concentrations [3]. ESI-FTICR-MS analyses were performed on T₀ and T₁₅ samples.

ESI-FTICR-MS analysis

ESI-FTICR-MS analysis was performed at the College of Science Major Instrumentation Cluster (COSMIC) Lab, Old Dominion University (Virginia, USA). The C₁₈ extraction method was used to concentrate DOM, which selectively retains non-polar, low-molecular-weight DOM (<700Da) [13]. Solid phase C₁₈ extraction disks (3M, Empore™, 47 mm diameter) were activated by LC-MS grade water and methanol before use. Sample waters were acidified to pH = 2 before passing through C₁₈ disks under vacuum. Water and methanol (both LC-MS grade) were used sequentially to elute materials retained on the C₁₈ disks. The eluates were collected, diluted with LC-MS grade water to a ratio of 50:50 (v/v) methanol:water for each sample.

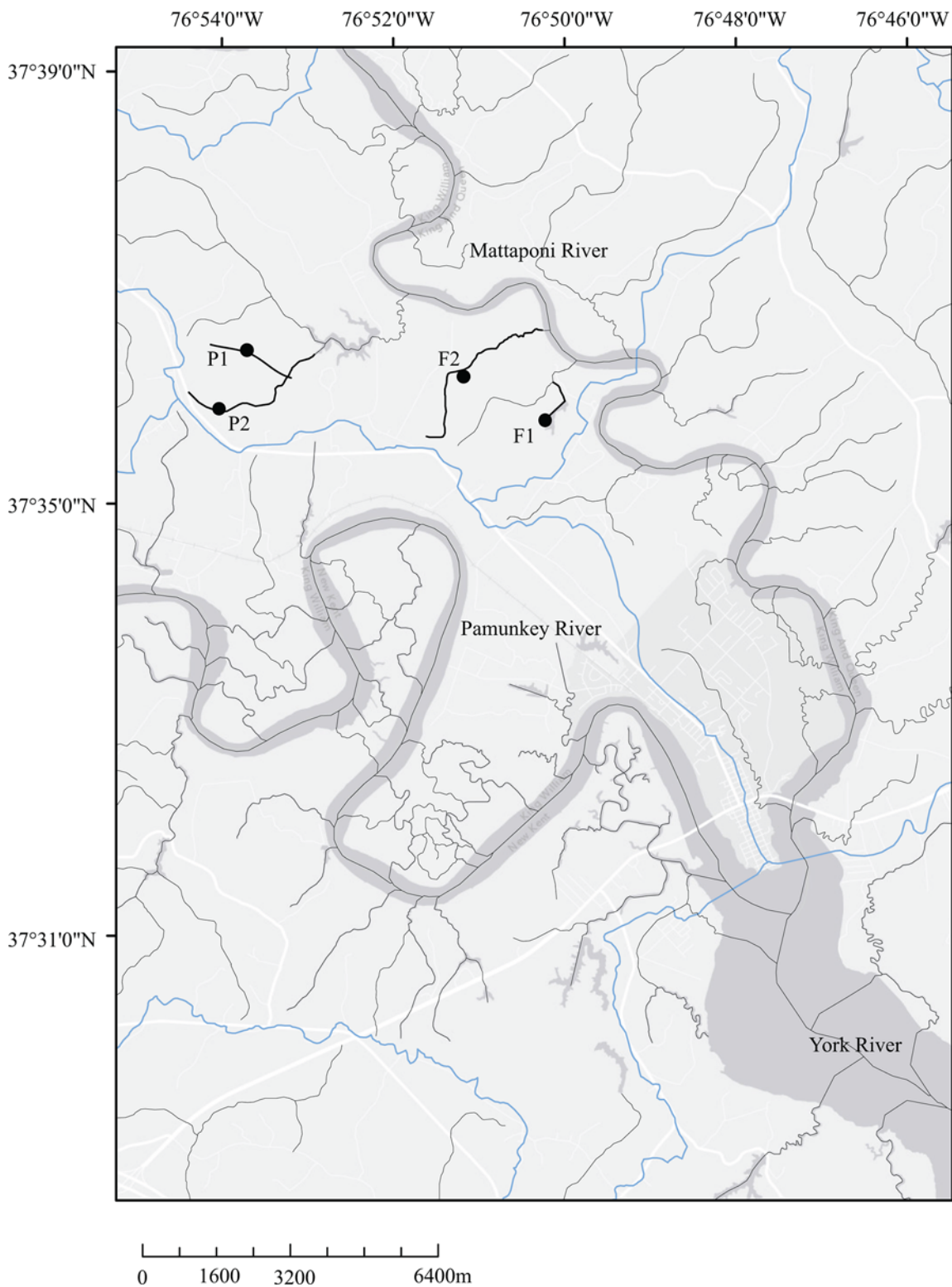


Fig 1. Map showing the study region and our sampling sites. Sampling streams are indicated by heavy black lines, and samples sites are indicated by solid black circles. Other streams in this area are denoted by gray lines, and the light blues lines are 12-digit HUC watershed boundaries.

doi:10.1371/journal.pone.0145639.g001

Table 1. Watershed land use, environmental parameters, and water parameters measured for the streams sampled in this study*.

Sampling site	Watershed land use composition	Water temperature (°C)	Specific conductivity (µS)	pH	Dissolved oxygen (mg/L)	DOC concentration (µM)	Water column chlorophyll-a (µg/L)	Nitrate (mg/L)	Ammonium (mg/L)	Sulfate (mg/L)
F1	100% forest	12.6	158.9	5	3.0	539	0.01	b.d.	b.d.	37.9
F2	100% forest	12.6	56.9	5	7.8	562	0.05	b.d.	b.d.	8.8
P1	70% pasture, 30% forest	12.6	210.4	6–7	7.9	675	0.14	2.29	2.49	14.4
P2	61% pasture, 39% forest	16.5	73.4	5	5.8	206	0.48	b.d.	b.d.	1.1

*b.d. = below detection; nitrate, ammonium, and sulfate were measured by using a Dionex ion chromatography.

doi:10.1371/journal.pone.0145639.t001

Ammonium hydroxide was then added to raise the sample pH to 8 in order to increase ionization efficiency [9].

All samples were continuously infused into an Apollo II ESI ion source of a Bruker Daltonics 12 Tesla Apex Qe FTICR-MS, using a syringe pump providing an infusion rate of 120µL/h. A solution of 0.1% ammonium hydroxide in 50:50 (v/v) LC-MS grade methanol: water was analyzed between each sample, serving as a blank to check for sample cross-contamination [14]. The samples and blanks were analyzed in negative ion mode, and electrospray voltages were made effective for each sample. Ions accumulated in a hexapole for 1.0 s before traveling to the ion cyclotron resonance cell. 300 or 350 transients were applied, yielding 4 mega word time-domain data for a total run time of 30 or 35 minutes, respectively. The summed free induction decay signal was zero-filled once and Sine-Bell apodized prior to fast Fourier transformation and magnitude calculation using the Bruker Daltonics Data Analysis software.

Formula assignments and data visualization and interpretation

All masses were internally calibrated following the calibration method described by Sleighter et al. [15], using fatty acid naturally present within our samples and other homologous peak series identified by Kendrick mass defect (KMD) analysis, which spanned the entire mass range of 200–700 m/z. Following the recommendation for data reproducibility [16], m/z values with signal to noise ratios ≥ 4 were considered for formula assignment. A molecular formula calculator developed at the FTICR-MS Facility at the National High Magnetic Field Laboratory of Florida State University (Molecular Formula Calc v.1.0 NHMFL, 1998) was used to generate empirical formulas. The range of the number of different atoms for each formula was set as 1–50 for carbon, 2–100 for hydrogen, 0–30 for oxygen, 0–6 for nitrogen, and 0–2 for sulfur.

Data processing followed the method described in detail by Sleighter and Hatcher [9] and Stubbins et al. [14]. Briefly, we selected chloride-free peaks whose measured mass and exact mass of empirical formulas were within ± 1 ppm, and then eliminated those empirical formulas that did not comply with the basic bonding criteria of organic compounds [7, 14, 17]: 1) $O/C \leq 1.2$; 2) $0.35 \leq H/C \leq 2.25$; 3) $N/C \leq 0.5$; 4) $S/C \leq 0.2$; 5) nitrogen rule (i.e., odd mass weight containing even-electron N ions, while even mass weight containing odd-electron N ions); and 6) Double Bond Equivalent (DBE) value being an integer ≥ 0 . The DBE is defined as:

$$DBE = (2 + 2 \times C - H + N + P) \div 2 \tag{1}$$

where C, H, N and P represent the number of carbon, hydrogen, nitrogen, and phosphorous

atoms in molecules, respectively. When multiple assignments were possible for a single m/z value, the formula was assigned based on homologous series [15, 18–19].

Van Krevelen (VK) analysis classifies the DOM molecules into different biochemical classes based on their H/C and O/C atomic ratios [20–21]. Following the classification described by Hockaday et al. and Ohno et al. [22–24], VK diagrams can be classified into six regions: 1) lipid-like region (H/C = 1.5–2.0, O/C = 0–0.3); 2) protein-like region (H/C = 1.5–2.2, O/C = 0.3–0.67); 3) lignin-like region (H/C = 0.7–1.5, O/C = 0.1–0.67); 4) carbohydrate-like region (H/C = 1.5–2.4, O/C = 0.67–1.2); 5) unsaturated hydrocarbon-like region (H/C = 0.7–1.5, O/C = 0–0.1); and 6) condensed aromatic ring structure (CAS) region (H/C = 0.2–0.7, O/C = 0–0.67) (Fig 2).

Additionally, several indices were used to classify DOM molecules with respect to their possible function groups. The modified aromaticity index (AI_{mod}), which assumes half of Os participating in a double bond, was used to identify aromatic formulas (AI_{mod} between 0.5 and 0.67) and CAS ($AI_{\text{mod}} > 0.67$, a more conservative way to define CAS than VK classification as described above) [25]:

$$AI_{\text{mod}} = \frac{1 + C - 0.5O - S - 0.5H}{C - 0.5O - S - N - P} \quad (2)$$

Formulas with $AI_{\text{mod}} < 0.5$ were classified as aliphatic and olefinic compounds such as alkanes, alkenes, alkanic acids, alenoic acids, alkanals, alkenals, and terpenes [26].

Statistical analysis

Jaccard similarity coefficients, which have been shown to be a powerful approach to compare FTICR-MS formulas across samples [27], were calculated to analyze formula similarity between different samples based on compound presence/absence, where coefficient = 1 indicates that two samples share the same formulas while coefficient = 0 indicates two samples having no formulas in common. Additionally, nonmetric multidimensional scaling (NMDS) was used to discern samples' similarities and dissimilarities. The imputing matrix was Bray-Curtis distance calculated according to compounds' presence/absence. This method has also been shown efficient in grouping samples in FTICR-MS studies [11, 28]. Reliability analysis was performed prior to NMDS (Cronbach's Alpha = 0.7; the two samples from the combined light+ bacteria incubations were removed to increase the value of Cronbach's Alpha), and three-dimension solution was used (Kruskal' stress = 0.01).

Results and Discussion

DOM formulas in T_0 samples

For T_0 samples, 1936–3083 compound peaks were assigned with molecular formulas, accounting for 64.5–70.8% of total peaks detected (Table 2). In all samples, CHO series dominated the formulas (71.8–87.9%), and other series made up minor fractions: CHOS (3.0–14.0%), CHON (2.9–9.2%), CHONS (0.2–2.0%), and CHOP (N,S) (1.4–6.3%) (Fig 3, S1 Appendix). The dominance of CHO molecular series has also been observed in other streams and rivers [11, 28]. The majority of compounds were aliphatic or olefinic (Table 2, Fig 2). Based on H/C and O/C ratios, 69.2% to 79.0% of total formulas can be classified as lignin (S3 Appendix), although these numbers were perhaps overestimated because many formulas fell in the aliphatic and olefinic region based on AI_{mod} (Fig 2), which is a more conservative method to identify aromatic molecules. The large abundance of lignin-like formulas agrees with the previous EEM-PARAFAC data on these samples showing the dominance of terrestrially-derived, humic and fulvic-like compounds in DOM [3], i.e., C10 and SQ1 peaks in the 13-component model [29]. Lignin

is found in the cell wall of vascular plants and is a major residual component of decomposed terrestrial plants [30–32]. Our observation supports the view that allochthonous inputs of OM serve as the primary source of food and energy to food webs in low-order streams [4, 33–34].

Aromatic compounds including CAS were concentrated in the CHO and CHON molecular series, while S and P-containing compounds were mostly olefinic or aliphatic (Fig 3). For CHON group, many formulas were not plotted in the protein-like region (i.e., $H/C = 1.5–2.2$, $O/C = 0.3–0.67$). A large majority (85–98%) of sulfur-containing formulas had O/S values ≥ 4 , perhaps suggesting that these formulas represented organosulfates. Comparing the distribution of molecular series across the T_0 samples, the only noticeable pattern was that F1 had a higher proportion and larger number of S-containing compounds than other samples (16% in F1 vs. 3.4–7.1% in other three samples; also see S1 Appendix), which could be due to a much higher sulfate concentration in this stream (37.9 mg/L in F1 vs. 1.1–14.4 mg/L in other streams, Table 1) that facilitated the formation of organosulfates.

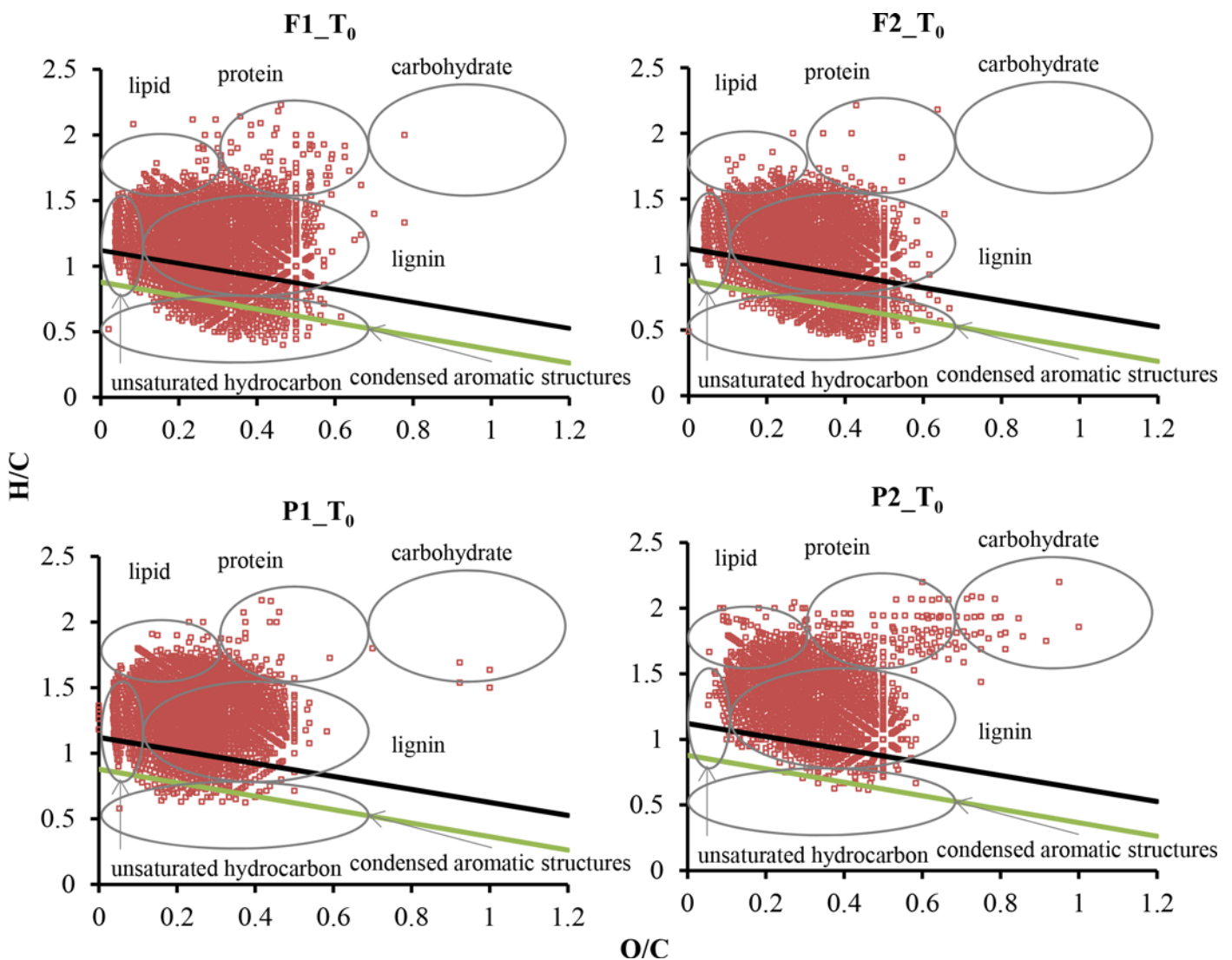


Fig 2. Van Krevelen diagrams of DOM at T_0 . The light green solid line denotes the regression line through the minimum H/C and O/C values for formulas with $Al_{mod} = 0.5$ (i.e., the majority of aromatic molecules are plotted below the line) and the black solid line denotes the regression line for formulas with $Al_{mod} = 0.67$ (i.e., the majority of CAS molecules are below the line).

doi:10.1371/journal.pone.0145639.g002

Table 2. FTICR-MS parameters of the forest and pasture stream DOM samples at T₀ and T₁₅.

Sample and Incubation Type	Time Point	Degradable DOC (%) [*]	#peaks detected [§]	#peaks with assigned formulas	Formulas in the CAS region	Al _{mod} between 0.5 and 0.67	Al _{mod} >0.67	(DBE) _m [§]	(O/C) _m [§]	(H/C) _m [§]	Refractory formulas
F1 Bacteria-only	T ₀	13.2	4357	3083	206 (6.7%)	767 (24.9%)	146 (4.7%)	11.01	0.30	1.17	85.7%
	T ₁₅		4313	3063	201 (6.6%)	616 (20.1%)	140 (4.6%)	11.17	0.30	1.17	
F2 Bacteria-only	T ₀	15.0	3704	2576	251 (9.7%)	686 (26.6%)	149 (5.78%)	11.65	0.31	1.13	79.0%
	T ₁₅		3681	2576	208 (8.1%)	463 (18.0%)	122 (4.74%)	10.94	0.34	1.14	
P1 Bacteria-only	T ₀	1.9	3878	2502	22 (0.9%)	291 (11.6%)	15 (0.60%)	9.74	0.26	1.30	32.0%
	T ₁₅		1978	1386	5 (0.4%)	36 (2.60%)	6 (0.43%)	8.40	0.37	1.34	
P2 Bacteria-only	T ₀	23.9	2746	1936	11 (0.6%)	146 (7.54%)	6 (0.31%)	8.79	0.31	1.34	69.7%
	T ₁₅		3403	2449	110 (4.5%)	335 (13.8%)	43 (1.76%)	9.91	0.34	1.23	
P1 Light + Bacteria	T ₀	15.9	3878	2502	22 (0.9%)	291 (11.6%)	15 (0.60%)	9.74	0.26	1.30	26.9%
	T ₁₅		1007	692	0 (0%)	5 (0.72%)	0 (0%)	7.61	0.30	1.39	
P2 Light + Bacteria	T ₀	50.0	2746	1936	11 (0.6%)	146 (7.54%)	6 (0.31%)	8.79	0.32	1.34	63.1%
	T ₁₅		2999	1916	0 (0%)	36 (1.88%)	0 (0%)	8.54	0.37	1.35	

* data from [3]

§ m/z in the range of 200–700; s/n ≥ 4; ratios (O/C)_m, (H/C)_m, and DBE_m were mean values from all peaks with assigned molecular formulas.

doi:10.1371/journal.pone.0145639.t002

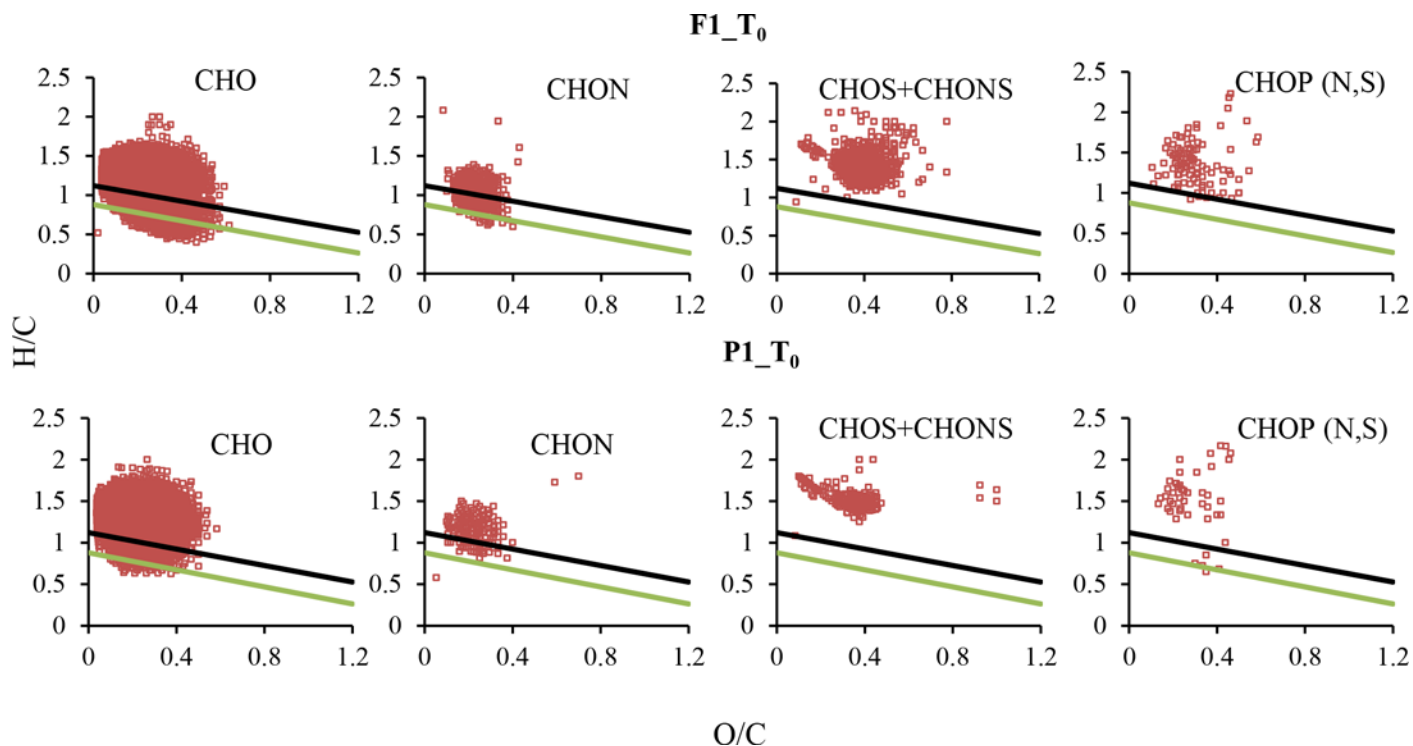


Fig 3. Van Krevelen diagrams for molecular series in F1 and P1 at T_0 . The light green solid line denotes the regression line through the minimum H/C and O/C values for formulas with $AI_{mod} = 0.5$ (i.e., the majority of aromatic molecules are plotted below the line) and the black solid line denotes the regression line for formulas with $AI_{mod} = 0.67$ (i.e., the majority of CAS molecules are below the line).

doi:10.1371/journal.pone.0145639.g003

Based on the Jaccard similarity coefficients of DOM formulas, the two forest stream samples (F1 and F2) were more similar than the two pasture stream samples (P1 and P2) (Fig 4). This observation was also echoed by the NMDS based on Bray-Curtis distance (Fig 5), where samples from the forest streams were plotted tightly into a small region, relative to more widespread samples from the pasture streams. DOM at T_0 from the pasture streams was characterized by lower mean DBE values (11.01 and 11.65 for the forest streams vs. 9.74 and 8.79 for the pasture streams), higher H/C values (1.17 and 1.13 for the forest streams vs. 1.30 and 1.34 for the pasture streams), and comparable O/C values (Table 2), indicating greater saturation for the formulas in the pasture streams. These patterns are in agreement with the results from VK classification and AI_{mod} analysis, showing DOM at T_0 from the pasture streams had lower numbers and percentages of aromatic formulas (Table 2, Fig 4). In addition to greater contributions of high-molecular-weight, aromatic compounds derived from land plants in the forest streams, these characteristics may be also related to light penetration, which was greater to the pasture streams due to removal of riparian trees in some sections of the pasture streams (*personal observation*). Light preferentially alters and remineralizes aromatic carbons with high DBE values [2, 14, 35].

FTICR-MS data cannot be used directly to derive information about compound abundance because of varied ionization efficiencies across compounds. Nevertheless, we found that the relative abundance of formulas in our samples largely agrees with the EEM-PARAFAC data from a companion study by Lu and colleagues [3]. EEM offers a relatively low resolution in compound separation and identification, but it is viewed as a technique capable of offering DOM compositional information in a quantitative manner [36, 37]. The higher percentages of aromatic formulas in F1 and F2 than in P1 and P2 (Table 2, Fig 4B) agree with the EEM data

showing that DOM from the forest streams had higher percent contributions of terrestrial fulvic and humic-like compounds than DOM from the pasture streams. Additionally, the EEM data showed that the percentages of protein-like DOM were lower in the forest streams, which was interpreted as evidence supporting that human activities likely increased autochthonous contributions of DOM. Similar patterns have been noted in many EEM studies of DOM in human-impacted streams and rivers [1, 2, 38]. However, this information cannot be derived from the FTICR-MS data. Although the relative abundance of formulas falling in the protein region (i.e., H/C = 1.5–2.2, O/C = 0.3–0.67) was higher in the pasture streams than in the forest streams (S3 Appendix), a large majority of these compounds did not contain N and cannot be classified as protein (Fig 3, S1 Appendix). Roth et al. [11] also reported that N-containing formulas were relatively lacking in surface water in comparison to soil water in a study employing

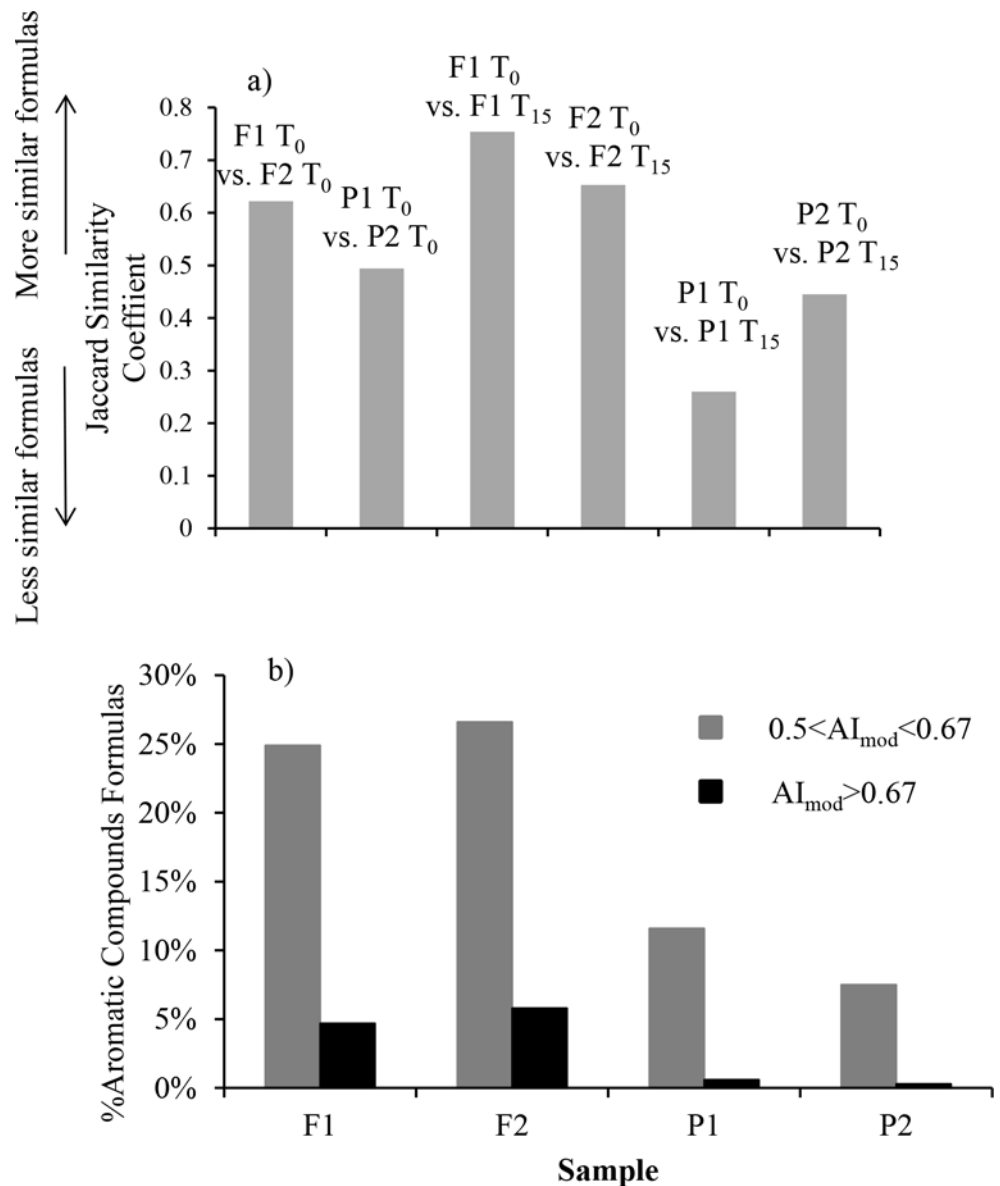


Fig 4. a) Jaccard similarity coefficients of DOM formulas between different samples or incubation time points; b) Relative abundance (%total formulas) of aromatic formulas in T₀ samples.

doi:10.1371/journal.pone.0145639.g004

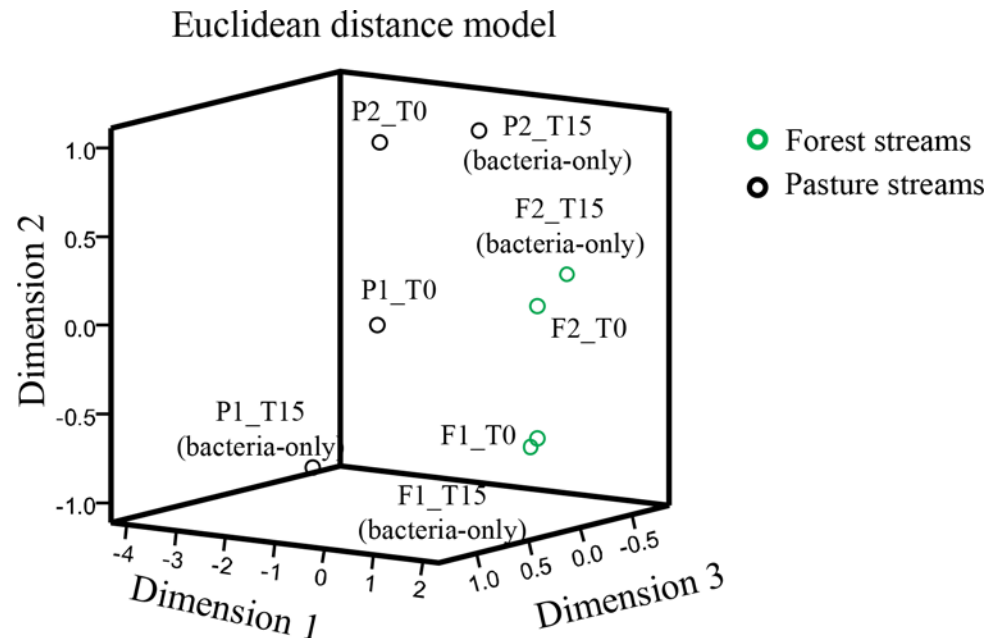


Fig 5. Nonmetric multidimensional scaling (NMDS) plot based on Bray-Curtis distances among the samples.

doi:10.1371/journal.pone.0145639.g005

the FTICR-MS technique, and explained this observation as a result of active microbial processing of N-containing compounds. Several reasons could account for the divergent observations from FTICR-MS and EEM measurements: 1) low retention of protein compounds by C_{18} filters, which was used for solid phase extraction prior to FTICR-MS analysis; and 2) possible overestimates of protein contribution by EEM measurements, on the basis that low molecular weight, N-free compounds such as gallic acid could also contribute to protein fluorescence peaks [39]. Divergent observations from FTICR-MS and EEM characterizations have also been recently noted by Stubbins et al. [14], who found that of the FTICR-MS formulas correlating to the classical protein-fluorescence peak in EEM-PARAFAC, only 31% contained N.

More CAS formulas were found in the forest streams than in the pasture streams (Table 2, Fig 2), based on both VK classification and AI_{mod} index. Black carbon, or charcoal, is an important source of molecules with CAS [22, 40–43], and they are produced by incomplete combustion of biomass and fossil fuels [44]. Therefore, the black carbon in DOM form the forest streams may be a result of controlled fire regularly used in the forested watersheds to suppress fuel buildup. This observation supports a recent contention that black carbon can be mobilized through dissolution and subsequently discharged to adjacent open water [43, 45].

Bacterial alterations to DOM compound formulas

In T_{15} compounds after the bacteria only-incubations, the relative abundance of molecular series exhibited distributions similar to T_0 samples, while no consistent pattern was observed among the samples with respect to changes in the relative abundance of molecular series (S1 Appendix). CHO series were still the most abundant group (73.7–84.6%) and the majority CHOS compounds (84.5–98.3%) had $O/S \geq 4$, indicating the presence of organosulfates. Furthermore, no consistent changes were observed in the relative proportions of aromatic compounds based on the AI_{mod} index analysis, despite that aromatic compounds were commonly

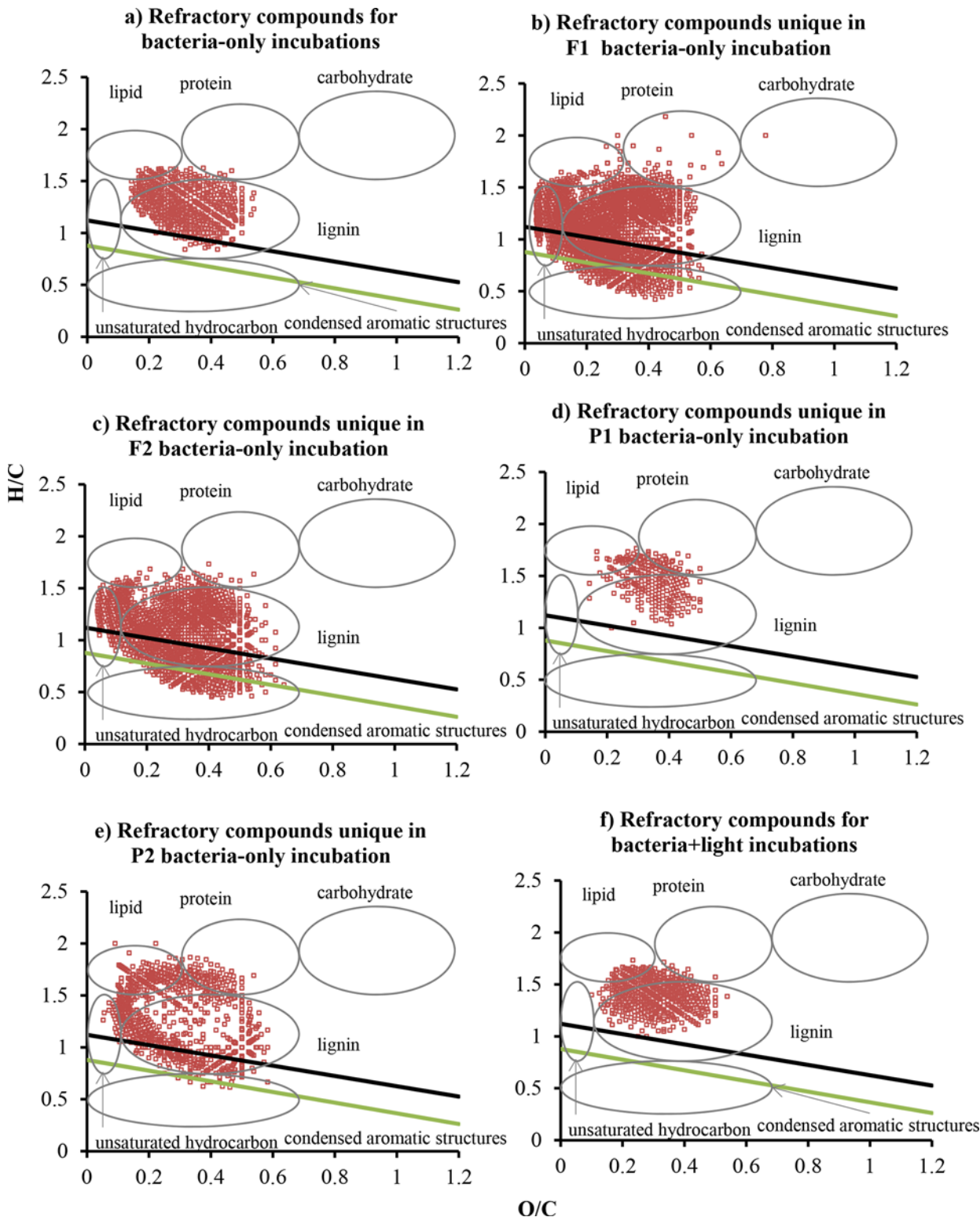


Fig 6. Van Krevelen diagrams of refractory compounds a) ubiquitous for all samples in bacteria-only incubations; b) unique in F1 bacteria-only incubation; c) unique in F2 bacteria-only incubation; d) unique in P1 bacteria-only incubation; e) unique in P1 bacteria-only incubation; and f) ubiquitous for all samples in combined bacteria+light incubations. The light green solid line denotes the regression line through the minimum H/C and O/C values for formulas with $Al_{mod} = 0.5$ (i.e., the majority of aromatic molecules are plotted below the line) and the black solid line denotes the regression line for formulas with $Al_{mod} = 0.67$ (i.e., the majority of CAS molecules are below the line).

doi:10.1371/journal.pone.0145639.g006

viewed as being more refractory to bacterial degradation [46]. F1, F2, and P1 showed a decrease in %aromatic formulas, while P2 showed an increase in %aromatic formulas (Table 2).

Two compound groups were evaluated by comparing DOM prior to and after the bacteria-only incubations: 1) biorefractory group that did not change during the incubations (i.e., present at T_0 and T_{15}); 2) bioreactive group that existed only at T_0 because they were remineralized or altered over the course of the incubations. Overall, DOM from the pasture streams had lower proportions of biorefractory formulas but higher proportions of bioreactive formulas than DOM from the forest streams (Table 2). This pattern agrees with the results from Jaccard similarity coefficient and NMDS analysis (Figs 4 and 5). The Jaccard similarity coefficients between T_0 and T_{15} samples were greater for DOM from the forest streams than from the pasture streams (Fig 4), and T_0 versus T_{15} samples were separated by smaller distances for the forest streams than for the pasture streams in the NMDS plot (Fig 5). Furthermore, the number of formulas was reduced by less than 1% for the two forest samples but changed by more than 26% for the two pasture samples (Table 2). These observations all show that the molecular compositions of the two pasture streams were altered to a greater extent than the two forest streams during the bacteria-only, dark incubations, with the caveat that P1 was different from the other three samples by demonstrating a large decrease in the number of compounds after the incubation. This decrease may be related more to higher nutrient concentrations in this sample (Table 1) than to DOM composition itself in stimulating microbial activity.

There were 567 compounds refractory to bacteria-only incubations (i.e., present in T_0 and T_{15} of all four samples, Fig 6A). These refractory compounds had H/C values ranging between 0.8 and 1.6 and O/C between 0.1 and 0.5, comparable to the ranges reported for formulas ubiquitously present across a range of ecosystems (river, forest, grassland, and bog), which were around 0.9–1.5 for H/C and 0.2–0.7 for O/C [11]. Biorefractory compounds unique to each sample varied from 235 and 2084, and they displayed larger ranges in both H/C and O/C ratios (Fig 6). Interestingly, the changes in the proportions of compounds falling in the protein-like and lipid-like regions showed the best correlation with the Jaccard similarity coefficients between T_0 versus T_{15} samples for the bacteria-only incubations (Fig 7), indicating that these compounds were primarily responsible for the changes in DOM molecules under the influences of bacterial processing. This is consistent with overall lower proportions of formulas in lipid-like and protein-like regions in biorefractory group ($8.0 \pm 5.2\%$ for lipid-like and $6.8 \pm 3.7\%$ for protein-like formulas) than in bioreactive group ($12.4 \pm 3.6\%$ for lipid-like and $12.3 \pm 7.9\%$ for protein-like formulas). Although the lability of proteins and lipids to microbial utilization has been widely reported in aquatic environments and soil extracts [47–50], the formulas identified by VK classification are not necessarily proteins or lipids. Instead, our observation argues for the lability of compounds with elemental makeup similar to proteins or lipids. Similarly, the H/C and O/C ranges of those resistant, ubiquitous compounds in various ecosystems reported by Roth et al. [11] did not include protein-like or lipid-like regions in VK diagrams. Furthermore, although a number of studies have noted a positive correlation between %biodegradable DOC versus %protein fluorescence [51–54], this correlation was not found in our study streams [3]. The FTICR-MS data here may provide an explanation—other formulas with high H/C ratios (>1.5) including those in lipid-like and unsaturated hydrocarbon-like regions also exhibited a positive correlation with the Jaccard similarity coefficients, indicating that they were also bioreactive and can play an important part in determining DOM biodegradability (Fig 7). This observation agrees with the previous finding that DOM with high H/C values was a labile source for bacteria, on the basis that H/C was a positive predictor of bacterial production in the Ogeechee River system [55]. Formulas in the carbohydrate-like region, however, did not show changes corresponding to changes in DOM formula similarity. This observation, rather than suggesting the refractory nature of carbohydrate-like compounds, is more likely a

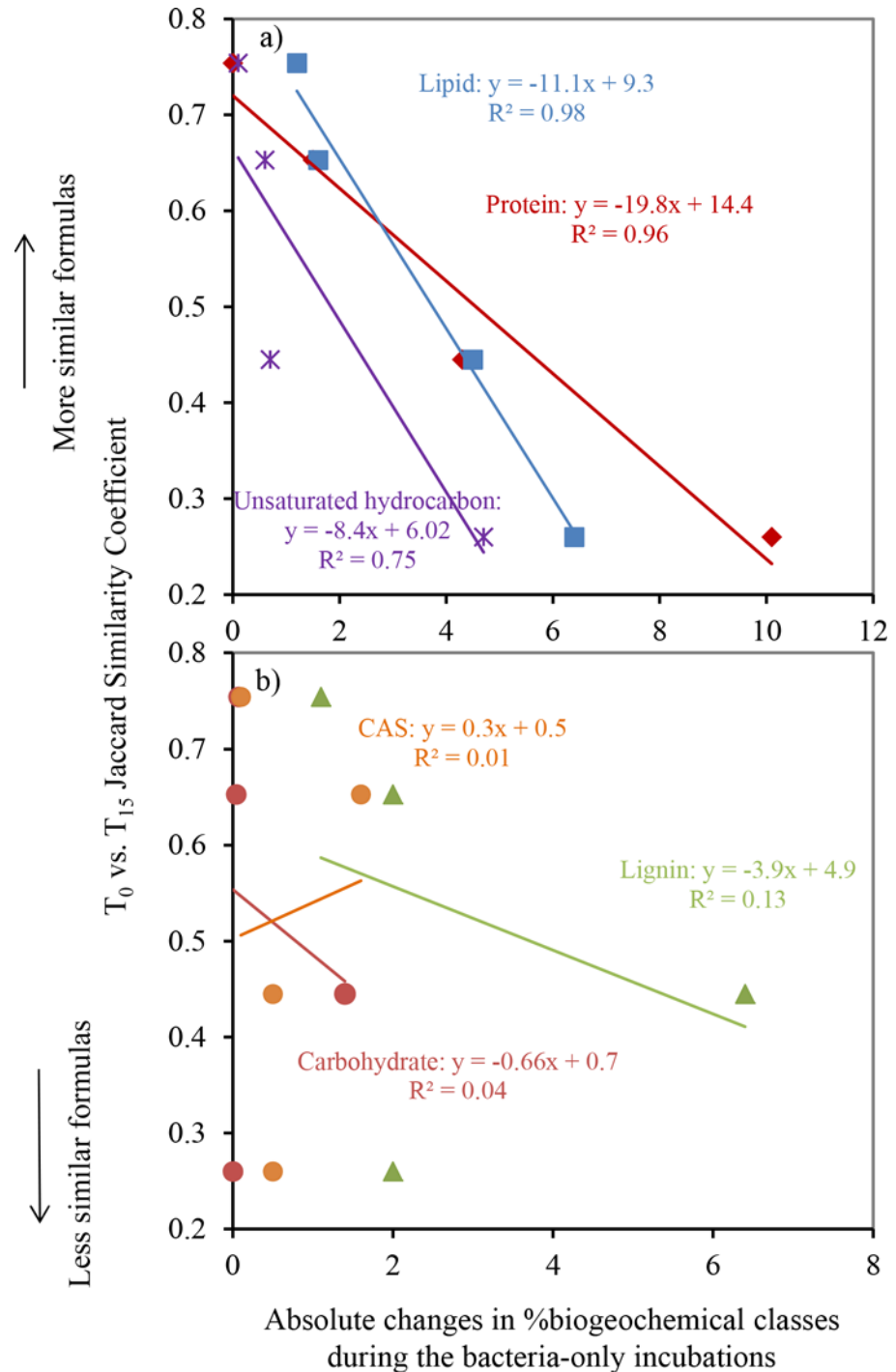


Fig 7. Correlations between Jaccard similarity coefficients and absolute changes in the proportions of the five Krevelen classified groups in the bacteria-only incubations. Solid lines represent linear trend lines.

doi:10.1371/journal.pone.0145639.g007

result of poor representation of carbohydrates in FT-ICRMS data related to their inefficient ionization in negative-mode ESI [14] and/or the selective retention of non-polar compounds through C₁₈ filters [13].

Combined light + bacteria alterations to DOM compound formulas

The two pasture stream samples were incubated under combined light and bacteria incubations. In both samples, the proportions of aromatic formulas and DBE decreased, and O/C values increased (Table 2). These characteristics are typical for light-induced DOM alterations, where the addition of oxygen to DOM during photochemical oxidation may be a result of ionization yielding hydrated electrons and organic radicals that both can react with molecular oxygen [35]. P1 and P2 shared 480 refractory compounds (present at both T_0 and T_{15} of combined light+bacteria incubations) which had H/C values varying from 1 to 1.7 and O/C values from 0.1 to 0.5 and comprised mostly aliphatic compounds (Fig 6). Relative to biorefractory compounds, they had higher values of H/C and lower values of AI_{mod} . Correspondingly, the relative percentages and absolute numbers of formulas falling in the region for unsaturated hydrocarbons were higher in reactive formulas (present only in T_0 of the combined incubations) than in refractory formulas— $7.1 \pm 0.6\%$ of reactive formulas versus $0.5 \pm 0.9\%$ of refractory formulas. These observations confirmed the sensitivity of unsaturated bonds (e.g., C = C, benzene rings, conjugate systems) to light alterations [14, 56–58]. Similar observations have been made for riverine and estuarine waters. For example, Kujawinski et al. [57] irradiated DOM samples from the Suwannee river with light of wavelengths >305 and >360 nm and found that DOM formulas with high DBE and low oxygen content were generally destroyed, resulting in lower unsaturation and higher oxygen content in residual DOM. Notably, all CAS formulas were removed after the combined bacteria+light incubations (Table 2), supporting the recent notion that black carbon mobilized from soil to water can be further altered by light [14, 22, 42, 45], as opposed to the conventional view that black carbon was inert in biogeochemical cycles due to the abundant content of aromatic and graphitic C [59–61]. In our experiments, the decomposition occurred within days, consistent with the previous finding that all black carbon-like formulas disappeared after 57 d photochemical incubations of Congo River DOM [14].

DOM similarity and diversity

The degree of alterations in DOM molecules indicated by the Jaccard similarity coefficient or Bray-Curtis distance did not correlate to %degradable DOC (Pearson $r \leq 0.03$, $P \geq 0.94$), indicating that heterotrophic microbes may be actively transforming DOM formulas without removing them through remineralization. This is not surprising as the similarity measures assess only compositional information (compound presence/absence) that does not always correspond to DOC quantity. Therefore, when interpreting DOM reactivity data from previous literature, one should keep in mind that degradable DOC, a widely used proxy to estimate DOM lability to microbes within lotic ecosystems [3, 62], may not always be an accurate proxy indicative of the actual roles of DOM in supporting microbial food webs. Likewise, Herlemann and colleagues [63] showed a decoupling between DOC concentration and DOM molecular composition, i.e., 4–10% DOC loss versus no significant changes in DOM molecular composition during 28-day incubation experiments.

We combined the number and similarity of DOM molecules to indicate DOM diversity. After the incubation experiments, the number of formulas decreased in all but one sample, but the majority samples showed decreases in similarity coefficients (Fig 8). In agreement with this pattern, T_{15} samples spread more widely than T_0 samples in the NMDS plot (Fig 5), indicating that light and/or bacterial processing led to more dissimilar DOM formulas. This is in contrast to the previous notion that DOM compounds become more uniform with increasing degrees of processing by light and bacteria, which was based primarily on the observation that photochemical and microbial processing of DOM tends to leave behind compounds with similar optical properties and carbon isotopic compositions across various systems (e.g., stream, river,

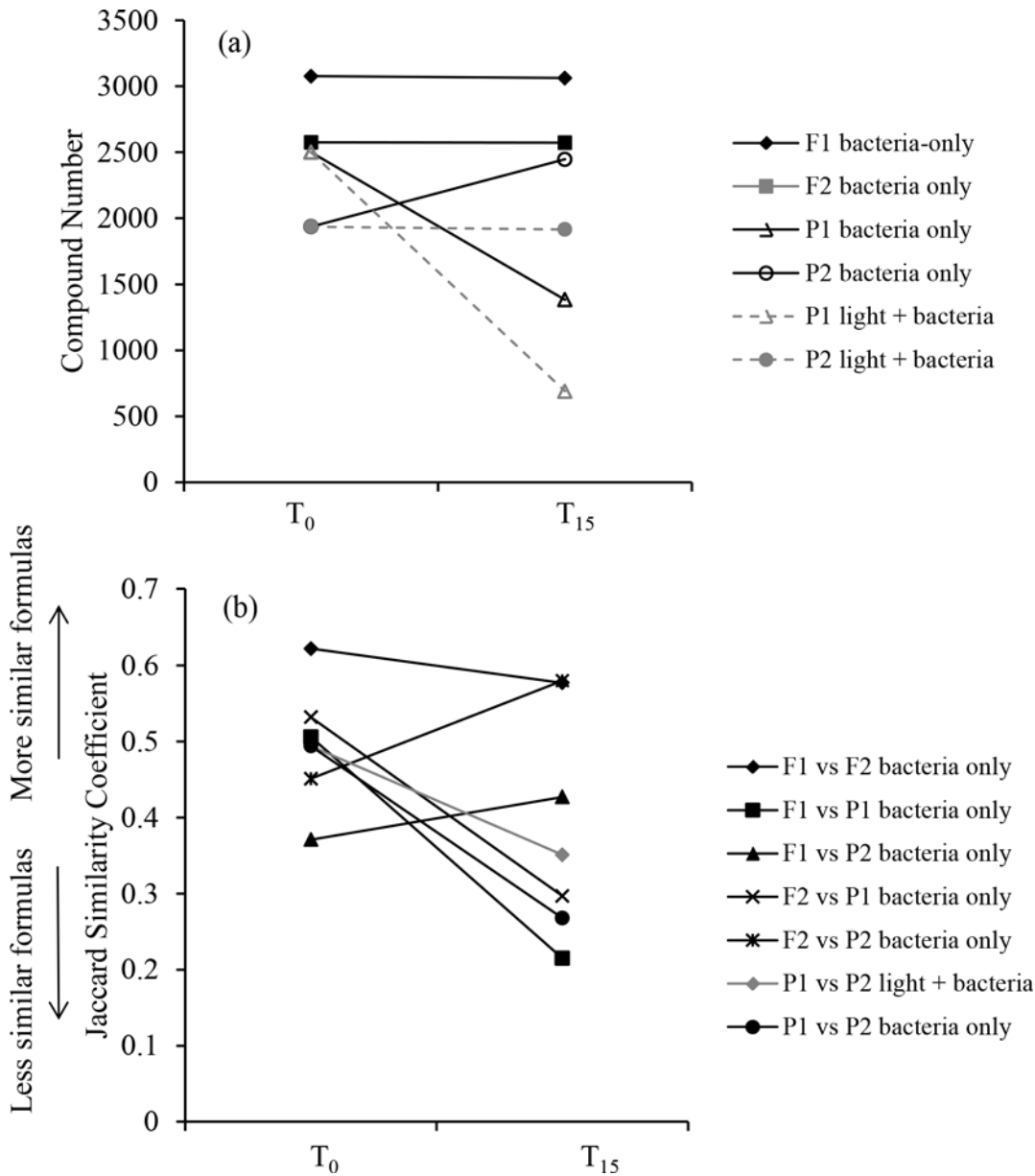


Fig 8. Comparing DOM diversity prior to versus after the incubations through a) compound number, and b) DOM formula similarities indicated by Jaccard similarity coefficients between T_0 vs. T_{15} samples.

doi:10.1371/journal.pone.0145639.g008

and coastal waters) and sample types (e.g., surface water and soil solutions) [3, 35, 48]. Our observations based on the FTICR-MS data remain to be verified and are unable to lead to generalizations on across-system patterns, largely due to the non-quantitative nature of this technique as well as the small sample size, which is a general feature for FTICR-MS studies owing to arduous efforts and expensive instruments involved. Nevertheless, these observations demonstrate the need to compare and synthesize high-resolution molecular data with isotopic and optical measurements to yield more reliable understanding on molecular transformations in lotic ecosystems.

Conclusions

Through the use of ESI-FTICR-MS, we characterized DOM from headwater streams draining pasture-dominated and forest-dominated watersheds, considering both molecular composition and molecular transformation under the influence of microbial and photochemical processes. In all the samples, the majority of the formulas fell within the lignin-like region, supporting the dominance of allochthonous DOM in headwaters. Formulas in the two forest streams were characterized by higher unsaturation and greater aromaticity than those in the two pasture streams, suggesting larger contributions of terrestrial plant-derived DOM in the forest streams. Larger numbers and percentages of CAS formulas were observed in the forest streams, indicating that soil black carbon resulting from controlled fires within the forest-dominated watersheds can be dissolved and discharged to open water. Bacterial processing altered DOM from the pasture streams to a greater extent than DOM from the forest streams, where formulas falling in the H/C and O/C ranges for protein-like, lipid-like, and unsaturated hydrocarbon-like regions were primarily responsible for DOM molecular alterations. During the combined light + bacteria incubations, more unsaturated compounds were preferentially degraded, and all CAS molecules were removed, supporting the lability of black carbon to photochemical alterations. Based on compound number and formula similarities, light and bacterial processing appeared to increase DOM formula diversity after the 15 d experiments. Overall, the use of FTICR-MS technique provided additional information unrevealed by previous measurements of DOC concentration, $\delta^{13}\text{C}$ -DOC, and fluorescence properties, demonstrating the importance of incorporating this sophisticated technique to identify qualitative changes in the sources and fates of terrestrially derived DOM in aquatic systems. However, interpreting FTICR-MS data from the perspective of extrapolating compound-level information to whole-DOM compositional information has to rely closely on other more quantitative measures such as fluorescence characterizations.

Supporting Information

S1 Appendix. The abundance and elemental ratio of various molecular series in each sample.

(DOCX)

S2 Appendix. Van Krevelen diagrams of refractory compounds unique for P1 and P2 in bacteria+light incubations

(PDF)

S3 Appendix. FTICR-MS parameters of the forest and pasture stream DOM samples at T_0 and T_{15} .

(DOCX)

S4 Appendix. Parameters for peaks with assigned formulas in T_0 samples.

(DOCX)

S5 Appendix. Parameters for peaks with assigned formulas in T_{15} samples (sample number continued from [S4 Appendix](#)).

(DOCX)

Acknowledgments

We thank Dr. B. Zhang for providing support for statistical analysis. This work was supported by a start-up analytical fund to Y. L. from the Department of Geological Science at the

University of Alabama, in collaboration with a Mellon Foundation Postdoctoral Fellow Grant from the College of William and Mary. We also acknowledge the HOOK's research fund and the Johnson travel fund from the Department of Geological Sciences, the University of Alabama, for providing student research and travel funds.

Author Contributions

Conceived and designed the experiments: YL JB RC EC. Performed the experiments: YL XL RM. Analyzed the data: XL YL RM. Contributed reagents/materials/analysis tools: YL JB RC EC PH. Wrote the paper: YL XL RM JB RC EC PH.

References

1. Wilson HF, Xenopoulos MA (2009) Effects of agricultural land use on the composition of fluvial dissolved organic matter. *Nature Geoscience* 2, 37–41.
2. Williams CJ, Xenopoulos MA, Yamashita Y, Jaffé R, Wilson HF (2010) Unraveling the role of land use and microbial activity in shaping dissolved organic matter characteristics in stream ecosystems. *Limnology and Oceanography* 55, 1159–1171.
3. Lu YH, Bauer JE, Canuel EA, Yamashita Y, Chambers RM, Jaffé R (2013) Photochemical and microbial alteration of dissolved organic matter in temperate headwater streams associated with different land use. *Journal of Geophysical Research-Biogeosciences* 118, 566–580.
4. Lu YH, Bauer JE, Canuel EA, Chambers RM, Yamashita Y, Jaffé R, et al. (2014) Effects of land use on sources and ages of inorganic and organic carbon in temperate headwater streams. *Biogeochemistry* 119, 275–292, doi: [10.1007/s10533-014-9965-2](https://doi.org/10.1007/s10533-014-9965-2)
5. Nebbioso A, Piccolo A (2013) Molecular characterization of dissolved organic matter (DOM): a critical review. *Analytical and Bioanalytical Chemistry* 405, 109–124. doi: [10.1007/s00216-012-6363-2](https://doi.org/10.1007/s00216-012-6363-2) PMID: [22965531](https://pubmed.ncbi.nlm.nih.gov/22965531/)
6. Kujawinski EB, Behn MD (2006) Automated analysis of electrospray ionization fourier transform ion cyclotron resonance mass spectra of natural organic matter. *Analytical Chemistry* 78, 4363–4373. PMID: [16808443](https://pubmed.ncbi.nlm.nih.gov/16808443/)
7. Mopper K, Stubbins A, Ritchie JD, Bialk HM, Hatcher PG (2007) Advanced instrumental approaches for characterization of marine dissolved organic matter: extraction techniques, mass spectrometry, and nuclear magnetic resonance spectroscopy. *Chemical Reviews* 107, 419–442. PMID: [17300139](https://pubmed.ncbi.nlm.nih.gov/17300139/)
8. Stubbins A, Lapierre JF, Berggren M, Prairie YT, Dittmar T, del Giorgio PA (2014) What's in an EEM? Molecular signatures associated with dissolved organic fluorescence in boreal Canada. *Environmental Science and Technology* 48, 10598–10606. doi: [10.1021/es502086e](https://doi.org/10.1021/es502086e) PMID: [25148241](https://pubmed.ncbi.nlm.nih.gov/25148241/)
9. Sleighter RL, Hatcher PG (2008) Molecular characterization of dissolved organic matter (DOM) along a river to ocean transect of the lower Chesapeake Bay by ultrahigh resolution electrospray ionization Fourier transform ion cyclotron resonance mass spectrometry. *Marine Chemistry* 110, 140–152.
10. Jaffé R, Yamashita Y, Maie N, Cooper WT, Dittmar T, Dodds WK, et al. (2012) Dissolved organic matter in headwater streams: compositional variability across climatic regions of North America. *Geochimica et Cosmochimica Acta* 94, 95–108, doi: [10.1016/j.gca.2012.06.031](https://doi.org/10.1016/j.gca.2012.06.031)
11. Roth VN, Dittmar T, Gaupp R, Gleixner G (2014) Ecosystem-specific composition of dissolved organic matter. *Vadose Zone Journal* 13, doi: [10.2136/vzj2013.09.0162](https://doi.org/10.2136/vzj2013.09.0162)
12. Leifer A (1988) *The Kinetics of environmental aquatic photochemistry: theory and practice*. Washington: American Chemical Society; 1988.
13. Kim S, Kramer RW, Hatcher PG (2003) Graphical method for analysis of ultrahigh-resolution broadband mass spectra of natural organic matter, the Van Krevelen diagram. *Analytical Chemistry* 75, 5336–5344. PMID: [14710810](https://pubmed.ncbi.nlm.nih.gov/14710810/)
14. Stubbins A, Chen H, Hatcher PG, Mopper K, Spencer RGM, Six J, et al. (2010) Illuminated darkness: molecular signatures of Congo River dissolved organic matter and its photochemical alteration as revealed by ultrahigh precision mass spectrometry. *Limnology and Oceanography* 55, 1467–1477.
15. Sleighter RL, McKee GA, Liu Z, Hatcher PG (2008) Naturally present fatty acids as internal calibrants for Fourier transform mass spectra of dissolved organic matter. *Limnology and Oceanography: Methods* 6, 246–251.
16. Sleighter RL, Chen H, Wozniak AS, Willoughby AS, Caricasole P, Hatcher PG (2012) Establishing a measure of reproducibility of ultrahigh-resolution mass spectra for complex mixtures of natural organic matter. *Analytic Chemistry* 84, 9184–9191.

17. Zhong J, Sleighter RL, Salmon E, McKee GA, Hatcher PG (2011) Combining advanced NMR techniques with ultrahigh resolution mass spectrometry: A new strategy for molecular scale characterization of macromolecular components of soil and sedimentary organic matter. *Organic Geochemistry* 42, 903–916.
18. Koch BP, Witt M, Engbrodt R, Dittmar T, Kattner G (2005) Molecular formulae of marine and terrigenous dissolved organic matter detected by electrospray ionization Fourier transform ion cyclotron resonance mass spectrometry. *Geochimica et Cosmochimica Acta* 69, 3299–3308.
19. Koch BP, Dittmar T, Witt M, Kattner G (2007) Fundamentals of molecular formula assignment to ultrahigh resolution mass data of natural organic matter. *Analytical Chemistry* 79, 1758–1763. PMID: [17297983](#)
20. Kim S, Simpson AJ, Kujawinski EB, Freitas MA, Hatcher PG (2003) High resolution electrospray ionization mass spectrometry and 2D solution NMR for the analysis of DOM extracted by C18 solid phase disk. *Organic Geochemistry* 34, 1325–1335.
21. Sleighter RL, Hatcher PG (2007) The application of electrospray ionization coupled to ultrahigh resolution mass spectrometry for the molecular characterization of natural organic matter. *Journal of Mass Spectrometry* 42, 559–574. PMID: [17474116](#)
22. Hockaday WC, Grannas AM, Kim S, Hatcher PG (2006) Direct molecular evidence for the degradation and mobility of black carbon in soils from ultrahigh-resolution mass spectral analysis of dissolved organic matter from a fire-impacted forest soil. *Organic Geochemistry* 37, 501–510.
23. Hockaday WC, Purcell JM, Marshall AG, Baldock JA, Hatcher PG (2009) Electrospray and photoionization mass spectrometry for the characterization of organic matter in natural waters: a qualitative assessment. *Limnology and Oceanography:Methods* 7, 81–95.
24. Ohno T, He Z, Honeycutt CW, Sleighter RL, Hatcher PG (2010) Ultrahigh resolution mass spectrometry and indicator species analysis to identify marker components of soil- and plant biomass-derived organic matter fractions. *Environmental Science and Technology* 44, 8594–8600. doi: [10.1021/es101089t](#) PMID: [20958002](#)
25. Koch BP, Dittmar T (2006) From mass to structure: An aromaticity index for high-resolution mass data of natural organic matter. *Rapid Communications in Mass Spectrometry* 20, 926–932.
26. Willoughby AS, Wozniak AS, Hatcher PG (2014) A molecular-level approach for characterizing water-insoluble components of ambient organic aerosol particulates using ultra-high resolution mass spectrometry. *Atmospheric Chemistry and Physics* 14, 10299–0314, doi: [10.5194/acpd-14-10393-2014](#)
27. Mosher JJ, Klein GC, Marshall AG, Findlay RH (2010) Geological influences of natural organic matter structure in stream waters by FT-ICR-MS. *Organic Geochemistry* 41, 1177–1188.
28. Kujawinski EB, Longnecker K, Blough NV, Del Vecchio R, Finlay L, Kitner JB, et al. (2009) Identification of possible source markers in marine dissolved organic matter using ultrahigh resolution mass spectrometry. *Geochimica et Cosmochimica Acta* 73, 4384–4399, doi: [10.1016/j.gca.2009.04.033](#)
29. Cory RM, McKnight DM (2005) Fluorescence spectroscopy reveals ubiquitous presence of oxidized and reduced quinones in dissolved organic matter. *Environ Science Technology* 39, 8142–8149, doi: [10.1021/Es0506962](#)
30. Bianchi TS, Canuel EA (2011) *Chemical biomarkers in aquatic ecosystems*. Princeton: Princeton University Press; 2011.
31. Kalbitz K, Solinger S, Park JH, Michalzik B, Matzner E (2000) Controls on the dynamics of dissolved organic matter in soils: A review. *Soil Science* 165, 277–304.
32. Kalbitz K, Kaiser K, Bargholz J, Dardenne P (2006) Lignin degradation controls the production of dissolved organic matter in decomposing foliar litter. *European Journal of Soil Science* 57, 504–516.
33. Aitkenhead-Peterson JA, McDowell WH, Neff JC (2003) Sources, production, and regulation of allochthonous dissolved organic matter inputs to surface waters. In: Findlay SEG, Sinsabaugh RL, editors. *Aquatic ecosystems: interactivity of dissolved organic matter*. Amsterdam: Academic Press; 2003. pp. 26–70.
34. Lu YH, Canuel EA, Bauer JE, Chambers RM (2014) Effects of watershed land use on sources and nutritional value of particulate organic matter in temperate headwater streams. *Aquatic Sciences* 76, 419–436, doi: [10.1007/s00027-014-0344-9](#)
35. Sulzberger B, Durisch-Kaiser E (2009) Chemical characterization of dissolved organic matter (DOM): A prerequisite for understanding UV-induced changes of DOM absorption properties and bioavailability. *Aquatic Sciences* 71, 104–126.
36. Jaffé R, McKnight DM, Maie N, Cory RM, McDowell WH, Campbell JL (2008) Spatial and temporal variations in DOM composition in ecosystems: The importance of longterm monitoring of optical properties. *Journal of Geophysical Research-Biogeosciences* 113, doi: [10.1029/2008JG000683](#)

37. Jaffé R, Cawley KM, Yamashita Y (2014) Applications of excitation emission matrix fluorescence with parallel factor analysis (EEM-PARAFAC) in assessing environmental dynamics of natural dissolved organic matter (DOM) in aquatic environments: a review. In: Rosario-Ortiz F, editor. *Advances in the physicochemical characterization of dissolved organic matter: impact on natural and engineered systems*. Washington DC: American Chemical Society; 2014. pp. 29–73.
38. Parr TB, Cronan CS, Ohno T, Findlay SEG, Smith SMC, Simon KS (2015) Urbanization changes the composition and bioavailability of dissolved organic matter in headwater streams. *Limnology and Oceanography* 60, 885–900, doi: [10.1002/lno.10060](https://doi.org/10.1002/lno.10060)
39. Maie N, Scully NM, Pisani O, Jaffé R (2007) Composition of a protein-like fluorophore of dissolved organic matter in coastal wetland and estuarine ecosystems. *Water Research* 41 (3), 563–570. PMID: [17187842](https://pubmed.ncbi.nlm.nih.gov/17187842/)
40. Cope MJ (1980) Physical and chemical properties of coalified and charcoaled phytoclasts from some British Mesozoic sediments: an organic geochemical approach to palaeobotany. *Physics and Chemistry of the Earth* 12, 663–677.
41. Baldock JA, Smernik RJ (2002) Chemical composition and bioavailability of thermally altered *Pinus resinosa* (Red pine) wood. *Organic Geochemistry* 33, 1093–1109.
42. Kim S, Kaplan LA, Benner R, Hatcher PG (2004) Hydrogen-deficient molecules in natural riverine water samples—evidence for the existence of black carbon in DOM. *Marine Chemistry* 92, 225–234.
43. Hockaday WC, Grannas AM, Kim S, Hatcher PG (2007) The transformation and mobility of charcoal in a fire-impacted watershed. *Geochimica et Cosmochimica Acta* 71, 3432–3445.
44. Goldberg ED (1985) *Black carbon in the environment: properties and distribution*. New York: John Wiley and Sons.
45. Jaffé R, Ding Y, Niggemann J, Vähätalo AV, Stubbins A, Spencer RGM, et al. (2013) Global charcoal mobilization from soils via dissolution and riverine transport to the oceans. *Science* 340, 345–347. doi: [10.1126/science.1231476](https://doi.org/10.1126/science.1231476) PMID: [23599492](https://pubmed.ncbi.nlm.nih.gov/23599492/)
46. McKnight DM, Hood E, Klapper L (2003) Trace organic moieties of dissolved organic materials in natural waters. In: Findlay SEG, Sinsabaugh RL, editors. *Aquatic ecosystems: interactivity of dissolved organic matter*. Amsterdam: Academic Press; 2003. pp. 71–91.
47. Harvey HR, Macko SA (1997) Kinetics of phytoplankton decay during simulated sedimentation: Changes in lipids under oxic and anoxic conditions. *Organic Geochemistry* 27, 129–140.
48. Kalbitz K, Schmerwitz J, Schwesig D, Matzner E (2003) Biodegradation of soil-derived dissolved organic matter as related to its properties. *Geoderma* 113, 273–291.
49. Kirchman DL (2003) The contribution of monomers and other low-molecular weight compounds to the flux of dissolved organic material. In: Findlay SEG, Sinsabaugh RL, editors. *Aquatic ecosystems: interactivity of dissolved organic matter*. Amsterdam: Academic Press; 2003. pp. 121–137.
50. Baldock JA, Masiello CA, Gelinas Y, Hedges JI (2004) Cycling and composition of organic matter in terrestrial and marine ecosystems. *Marine Chemistry* 92, 39–64.
51. Balcarczyk KL, Jones JB Jr, Jaffé R, Maie N (2009) Stream dissolved organic matter bioavailability and composition in watersheds underlain with discontinuous permafrost. *Biogeochemistry* 94, 255–270.
52. Fellman JB, Hood E, D'Amore DV, Edwards RT, White D (2009) Seasonal changes in the chemical quality and biodegradability of dissolved organic matter exported from soils to streams in coastal temperate rainforest watersheds. *Biogeochemistry* 95, 277–293, doi: [10.1007/s10533-009-9336-6](https://doi.org/10.1007/s10533-009-9336-6)
53. Fellman JB, Hood E, Edwards RT, D'Amore DV (2009) Changes in the concentration, biodegradability, and fluorescent properties of dissolved organic matter during stormflows in coastal temperate watersheds. *Journal of Geophysical Research-Biogeosciences* 114, doi: [10.1029/2008JG000790](https://doi.org/10.1029/2008JG000790)
54. Hosen JD, McDonough OT, Febria CM, Palmer MA (2014) Dissolved organic matter quality and bioavailability changes across an urbanization gradient in headwater streams. *Environ Science and Technology* 48 (14), 7817–7824, doi: [10.1021/Es501422z](https://doi.org/10.1021/Es501422z)
55. Sun L, Perdue EM, Meyer JL, Weis J (1997) Use of elemental composition to predict bioavailability of dissolved organic matter in a Georgia river. *Limnology Oceanography* 42, 714–721.
56. Schmitt-Kopplin P, Hertkorn N, Schulten HR, Kettrup A (1998) Structural changes in a dissolved soil humic acid during photochemical degradation processes under O-2 and N-2 atmosphere. *Environmental Science and Technology* 32, 2531–2541.
57. Kujawinski EB, Del Vecchio R, Blough NV, Klein GC, Marshall AG (2004) Probing molecular-level transformations of dissolved organic matter: insights on photochemical degradation and protozoan modification of DOM from electrospray ionization Fourier transform ion cyclotron resonance mass spectrometry. *Marine Chemistry* 92, 23–37.
58. Dalzell BJ, Minor EC, Mopper KM (2009) Photodegradation of estuarine dissolved organic matter: a multi-method assessment of DOM transformation. *Organic Geochemistry* 40, 243–257.

59. Skjemstad JO, Clarke P, Taylor JA, Oades M, McClure SG (1996) The chemistry and nature of protected carbon in soils. *Australian Journal of Soil Research* 34, 251–271.
60. Glaser B, Haumaier G, Guggenberger G, Zech W (1998) Black carbon in soils: the use of benzene carboxylic acids as specific markers. *Organic Geochemistry* 29, 811–819.
61. Major J, Lehmann J, Rondon M, Goodale C (2010) Fate of soil-applied black carbon: downward migration, leaching and soil respiration. *Global Change Biology* 16, 1366–1379.
62. Wilson HF, Saiers JE, Raymond PA, Sobczak WV (2013) Hydrologic drivers and seasonality of dissolved organic carbon concentration, nitrogen content, bioavailability, and export in a forested New England stream. *Ecosystems* 16 (4):604–616, doi: [10.1007/s10021-013-9635-6](https://doi.org/10.1007/s10021-013-9635-6)
63. Herlemann DPR, Manecki M, Meeske C, Pollehne F, Labrenz M, Schulz-Bull D, et al. (2014) Uncoupling of bacterial and terrigenous dissolved organic matter dynamics in decomposition experiments. *PIOS ONE* 9 (4), doi: [10.1371/journal.pone.0093945](https://doi.org/10.1371/journal.pone.0093945)